Arabian Journal of Chemistry (2014) 7, 1124–1130

King Saud University

Arabian Journal of Chemistry

www.ksu.edu.sa
www.sciencedirect.com

ORIGINAL ARTICLE

Theoretical investigation on homoleptic Yttrium tri-guanidinates

Salima Lakehal [a,b], Nadia Ouddai [a,*], Mohamed Bououdina [c,d]

[a] Laboratoire Chimie des matériaux et des vivants, Activité, Réactivité Université Hadj Lakhdar, Batna 05000, Algeria
[b] Department of Materials Sciences, Faculty of Sciences, University of Oum el Bouaghi, Oum el Bouaghi 04000, Algeria
[c] Nanotechnology Centre, University of Bahrain, P.O. Box 32038, Bahrain
[d] Department of Physics, College of Science, University of Bahrain, P.O. Box 32038, Bahrain

Received 31 August 2012; accepted 12 March 2013
Available online 22 March 2013

KEYWORDS
DFT;
TDDFT;
Guanidinate;
Yttrium;
HOMO;
LUMO

Abstract The electronic and molecular structures of the homoleptic Yttrium tris-guanidinates complexes $Y[(N^iPr)_2CNR_1R_2]_3$, [R_1 = R_2 = Me, Et and iPr] have been investigated employing DFT calculations in order to understand the structures, bonding and energies of the interactions between Yttrium metal and guanidinate ligands. The effect of the substitution on nitrogen position of guanidinate in these complexes has been also investigated employing DFT and TDDFT calculations for six kinds of models obtained by alternative substitution of alkyl on nitrogen of the guanidinate ligands. The results reveal that the substitution position plays a crucial role in the geometric structure by affecting the torsion angle and the HOMO–LUMO transitions. The energy decomposition analysis indicates a majority of ionic bonding in all systems; the exception is in the M4 ($Y[(N_YR)_2CN_CR_1R_2]_3$; R = Et and R_1 = R_2 = H) which present a significant degree of covalency.

1. Introduction

In recent years guanidinate ligands, an isoelectronic alternative to cyclopentadienyl ligands, have attracted increasing attention as ancillary ligands in the coordination and organolanthanide chemistry, as well as providing tuneability in terms of steric and electronic properties by variation of the substituents R, R_1 and R_2 on the nitrogen atoms (see Scheme 1). It is found that the above guanidinate ligands are efficient catalysts in homogeneous catalyzes such as the polymerization of nonpolar and polar monomers, e.g., ethylene, propylene, (Trifonov et al., 2006) styrene, (Luo et al., 2002; Ajellal et al., 2008), and lactones (lactide and ε-caprolactone), (Yao et al., 2003; Giesbrecht et al., 2001) as well as hydrosilylation of alkenes (Ge et al., 2008) and methyl methacrylate polymerization (Skvortsov et al., 2007). Furthermore, the bidentate chelating effect of the guanidinate ligands is expected to enhance the thermal/chemical stability of the resulting metal complexes and thus make them suitable precursors for metal–organic chemical vapor deposition (MOCVD) and atomic laser

* Corresponding author.
E-mail address: ouddai_nadia@yahoo.fr (N. Ouddai).
Peer review under responsibility of King Saud University.

ELSEVIER Production and hosting by Elsevier

1878-5352 © 2013 Production and hosting by Elsevier B.V. on behalf of King Saud University.
http://dx.doi.org/10.1016/j.arabjc.2013.03.004

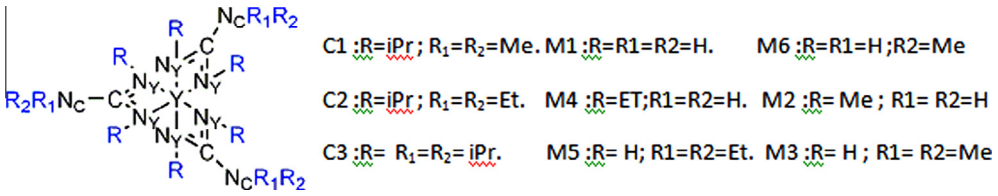

Scheme 1 Atom labeling scheme used.

deposition (ALD) (Milanov et al., 2009). To date, a very few homoleptic tris-guanidinate rare-earth complexes have been reported in the literature (Chen et al., 2004; Zhou et al., 2005, 2004; Pang et al., 2005). Very recently, Milanov et al. synthesized homoleptic rare-earth guanidinate complexes, and studied their structure and reactivity in order to evaluate them as precursors for MOCVD and ALD of rare-earth oxide films (Milanov et al., 2008).

In the present study, a systematic examination by relativistic density functional theory (DFT) and time-dependent DFT (TDDFT) of the electronic structures, ligand effects and optical properties of several Yttrium guanidinate complexes, with methyl, ethyl and isopropyl as guanidinate ligands was performed.

The theoretical models were first presented and described in detail and then a new computational set up with the application of quantum relativistic DFT methods was presented. A summary of the new findings will be presented then compared with some experimental results and finally their possible impacts on the understanding of guanidinate bonding are discussed.

2. Computational method and description of the studied systems

Density functional theory calculations were carried out using the Amsterdam Density Functional (ADF) program developed by Baerends et al. (1973). Electron correlation was treated within general gradient approximation using the PW91 functional (Perdew et al., 1992). The atom electronic configurations were described by a triple ζ Slater type orbital (STO) basis set for H 1s, and 2s and 2p for C and N, augmented with 2p single-ζ polarization functions for H atoms, with 3d single- ζ polarization functions for C and N. The atomic basis set of Yttrium is a triple ζ -STO for the outer 4d and 5s orbitals and a frozen core approximation for the shells of lower energy. Relativistic corrections were taken into account with the use of the relativistic scalar zero-order-regular approximation (ZORA) method (van Lenthe et al., 1999). The integration parameter, the energy convergence criterion and the cutoff were set to be 5, 10^{-3} au and 0.4, respectively.

The bonding interactions in Y-guanidinate have been analyzed by means of Morokuma-type energy decomposition analysis (decomposition of the bonding energy into the Pauli (exchange) repulsion, total steric interaction, and orbital interaction terms) (Bickelhaupt et al., 2000) developed by Ziegler and Rauk for DFT methods and incorporated in ADF (Ziegler and Rauk, 1979). For these complexes, we have selected Y^{+3} and 3[gun]$^{-}$ as a reference fragments in their appropriate geometry. This choice is focusing purely on the Y-guanidinate bonding. X-ray single crystal structures of the Yttrium tri-guanidinates complexes were used like a starting point, with our optimizations for: C3, C2 and C1 (Milanov et al., 2008). We also tested a total optimization of M1 by taking the X-ray single structure of C3 like the starting point.

In this work, the systems of interest are of general formula $Y[(N_YR)_2CN_CR_1R_2]_3$, (Scheme 1) where R_1 and R_2 are the alkyl grouping of the nitrogen atom of guanidinate, nonbonding to metal; be it the N_C position, and R is the alkyl group of the nitrogen atom of guanidinate, directly related to metal; be it the N_Y position (see Scheme 1). It seemed interesting to study the electronic influence of the ligands surrounding the guanidinate. The optimizations of these complexes were carried out starting from the X-ray single crystal structures data already available in the literature (Milanov et al., 2008). The experimental crystal structures were completely optimized without any constraints. The model systems must be first of all sufficiently close to the experimental complexes to allow comparisons and thus validate the theoretical approach.

In the first proposed model, the hydrogen atoms replace advantageously the isopropyl ligand and the objective is to design lighter models which require a less computing time by preserving the targeted physicochemical properties.

3. Results and discussion

3.1. Geometrical analysis

The Yttrium tri-guanidinates coordination sphere in all complexes can be described as being constituted of two triangles N(1)–N(2)–N(3) and N(4)–N(5)–N(6). We consider the torsion angle θ = N(3)–T(1)–T(2)–N(5) between the two planes N(3)N(2)N(1) and N(5)N(4)N(6), those that are formed by the six guanidinate backbone N atoms (T(1) and T(2) are the centroids of the two planes, see Scheme 2). For an ideal trigonal prism this torsion angle is expected to be 0°. The geometry around the Yttrium ions can be described as a distorted trigonal prism, according to the θ values presented in Table 1.

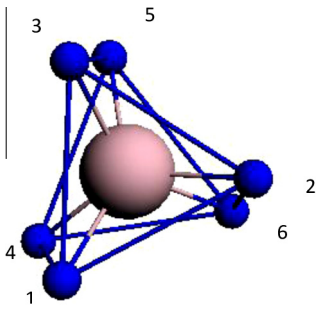

Scheme 2 Distorted trigonal prism arrangement of nitrogen atoms coordinated to Yttrium.

Table 1 Selected structural parameters of the optimized structures.

	$Y–N_Y$	$C–N_y$	$C–N_C$	$N_Y–Y–N_Y$	$N_Y–C–N_Y$	$Y–N_Y–C$	$R_1–N_C–R_2$	θ
C1	2.43 (2.368)	1.345*(1.334)*	1.405 (1.396)	55.8 (56.7)	115.6 (115.2)	94.3	115.8 (116)	16.0
C2	2.429 (2.377)	1.345 (1.338)	1.408 (1.412)	55.8 (56.93)	115.3 (115.8)	94.4	118.7 (118)	16.7
C3	2.424 (2.364)	1.346 (1.348)	1.417 (1.426)	55.7 (56.9)	114.5 (113.7)	94.9	124.9 (128)	18.0
M1	2.372	1.337	1.399	57.0	115.8	93.7	111.5	18.8
M2	2.371	1.341	1.390	57.2	115.9	93.4	113.3	19.6
M3	2.373	1.343	1.394	56.9	114.6	94.1	116.7	18.6
M4	2.376	1.342	1.392	57.1	115.6	93.6	113.4	21.2
M5	2.368	1.345	1.393	56.9	114.5	95.1	117.2	19.0
M6	2.374	1.337	1.390	57.0	115.6	93.5	115.2	18.7

The optimized geometrical parameters and the available experimental data are summarized in Table 1 (The values given in parentheses are the crystallographic data). Indeed, the structures obtained are not significantly different from those of the experimental complexes; the bonds lengths are in agreement with the experimental distances, the $Y–N_Y$ distances are overestimated of 0.058 Å on average than those of the experimental values. A similar overestimation was also reported earlier (Wang et al., 2004); such an overestimation may have resulted as a consequence of the selected theoretical method and molecular systems chosen in our present investigation. Comparing the substitution on the two positions (N_Y and N_C), it is noted that $Y–N_Y$ and $C–N_C$ bond lengths decreases slightly by increasing the alkyl group on N_Y position and increases by increasing the alkyl group on N_C position in the following order:

$$C1 > C2 > C3 \quad M3 > M5 \quad M2 > M4$$

All complexes angles are well reproduced with a maximum difference of 4° of the $R_1–N_C–R_2$ angle. The angles variations $N_Y–Y–N_Y$, $N_Y–C–N_Y$ and $Y–N_Y–C$ are negligible (deviation from 0.2° to 1.2°, not very significant values on this level of theory and modeling); but the deviation on the $R_1–N_C–R_2$ angle is more remarkable with variations of 1.8, 5.2, 1.9, 5.7 and 3.9° (compared to M1 values) from M2 to M6 respectively. This deviation is due to the increase in the dialkylamino group.

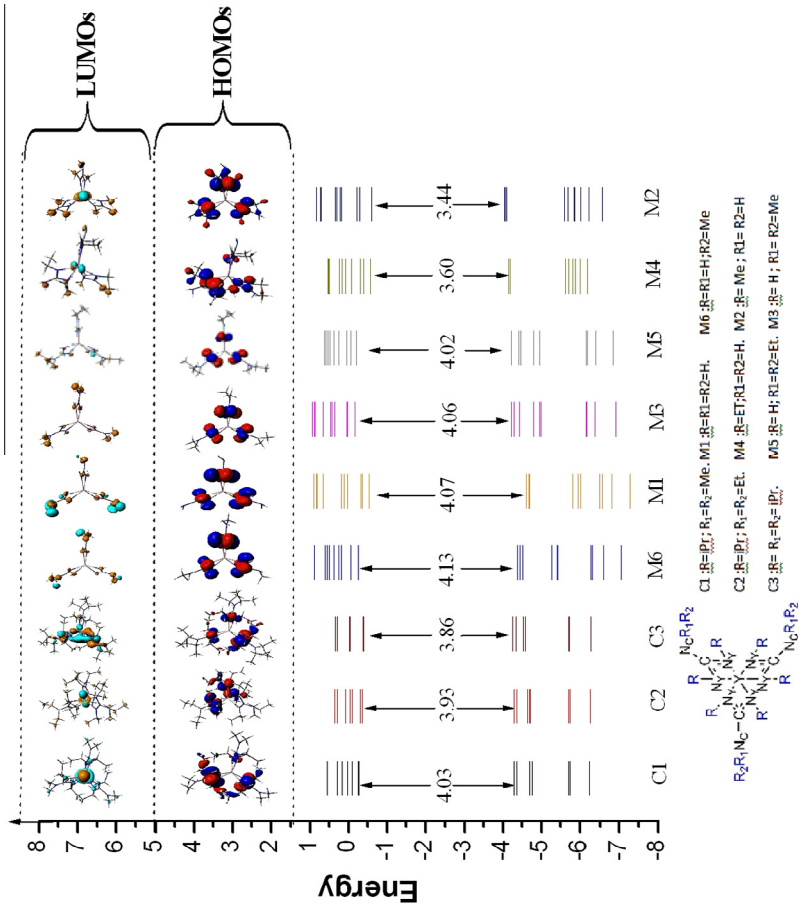

Figure 1 Comparative MO diagrams of the studied systems.

Table 2 Energies (eV) and torsion angles (°).

	E_{HOMO}	E_{LUMO}	$\Delta E_{HOMO-LUMO}$	E_{TOTAL}
C1	−4.290	−0.260	4.030	−547.75
C2	−4.278	−0.349	3.930	−647.15
C3	−4.259	−0.396	3.860	−745.79
M1	−4.602	−0.525	4.077	−155.34
M2	−4.039	−0.600	3.439	−252.87
M3	−4.224	−0.166	4.058	−252.76
M4	−4.152	−0.564	3.588	−352.36
M5	−4.222	−0.200	4.022	−352.12
M6	−4.380	−0.252	4.128	−189.54

This result is well confirmed by the experimental data (see Table 1). It can be seen that, for complexes having the same substitution position the torsion angle increases in the order C3 > C2 > C1, M5 > M3 and M4 > M2. An increase in the degree of geometric distortion with increasing the dialkylamido group (Me_2N < Et_2N < iPr_2N) of the guanidinate ligand is evident (see Table 1). The value of θ for M4 is found to be 21.2° which presents the most distorted trigonal prism.

3.2. Molecular orbital analysis

The molecular orbital diagrams obtained for the three synthesized complexes as well as the various optimized models 1–6 are compared in Fig. 1. In all cases, a large energy gap separates the occupied orbital block from a vacant one. M6 presents the largest gap with a value of 4.13 eV. It can be also noted that the highest occupied molecular orbital (HOMO) – lowest unoccupied molecular orbital (LUMO) gap calculated for M3 (4.06 eV) and M5 (4.02 eV) is higher than that calculated for M2 (3.44 eV) and M4 (3.60 eV), respectively Table 2. This gap is proportional with the increase in the alkyl chains, substituted on N_Y position (M4 and M2) and is inversely proportional to the same substitution on N_C position (Me, Et and *i*Pr, M3 and M5). For the synthesized compounds, it is noted that there are four separated occupied orbitals among the others, which makes their oxidation very difficult, compared to M2 and M4 which have only two orbitals. The composition of a selection of OM located in the area HOMO–LUMO for the complexes studied here is given in (SI. 1). The participation of the various nitrogen atoms of the guanidinate is almost homogeneous with a maximum contribution of 98% accompanied by a weak contribution of 2%, 2%, 1% and 2% for model 1–3 and, 6 respectively of the metal atom.

3.3. Charge analysis

The study of the atomic net charge by Hirshfeld analysis (Hirshfeld, 1977), these species (see Table 3) show that the nitrogen atom N_C is negatively charged than N_Y. The metal charge increases slightly with the increase of alkyl chain and is higher on the C1 complex.

3.4. Energetic analysis

The ionic and covalent character of coordination bond dominates a crucial role in coordination chemistry, which naturally depends on metal and ligands. The chemical description of the

Table 3 Hirshfeld charge analysis.

	Y	N_Y	C	N_C	Δ (Y–N_Y)	Δ (C–N_C)
C1	0.650	−0.203	0.133	−0.053	0.447	0.080
C2	0.646	−0.204	0.133	−0.058	0.442	0.075
C3	0.641	−0.202	0.133	−0.060	0.439	0.073
M1	0.632	−0.287	0.130	−0.186	0.345	0.056
M2	0.624	−0.217	0.131	−0.171	0.407	0.040
M3	0.611	−0.290	0.129	−0.054	0.321	0.075
M4	0.612	−0.214	0.132	−0.171	0.398	0.039
M5	0.610	−0.290	0.130	−0.048	0.320	0.082
M6	0.622	−0.280	0.127	−0.118	0.342	0.009

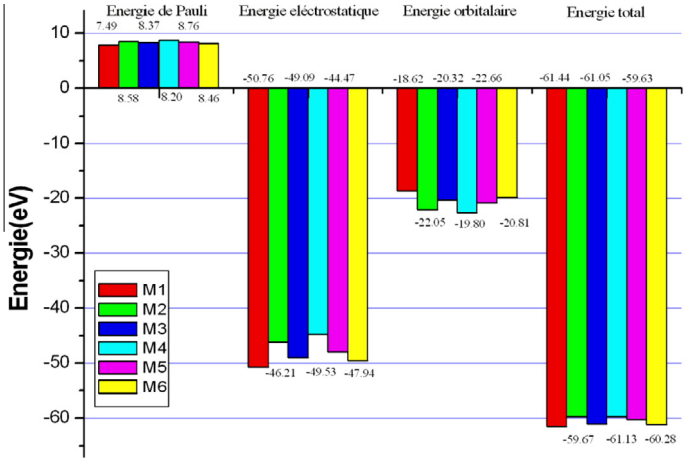

Figure 2 Various energy contributions.

Table 4 Percentage of electrostatic and orbital contributions to the Y-guanidinate bonding.

	M1	M2	M3	M4	M5	M6
% Eorb	26.8	32.3	29.3	33.6	30.3	28.5
% Eelec	73.2	67.7	70.7	66.4	69.7	71.5

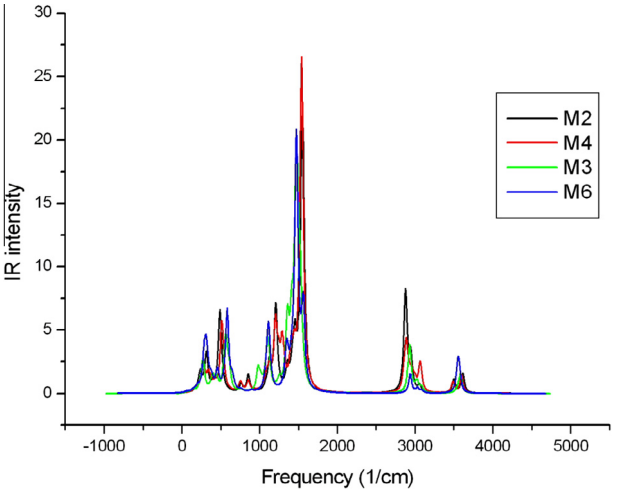

Figure 3 Theoretical vibrational spectra of M2, M3, M4 and M6.

metal–ligand interaction of the bonding characteristics, viz., ionic versus covalent, is one of the challenging problems in metallic complexes. The ionic and covalent characteristics of organic complexes are associated with the binding nature of metal with ligand. Hence, in the framework of DFT, the approach of energy diagram decomposition developed by Ziegler and Rauk (1979) has been proposed to describe qualitatively the ionic and covalent character of metal–ligand bond.

In this study, the three ligands of guanidinate in their optimized position within the complex are introduced as a single fragment (3guan), and the interaction of such a fragment (3guan) with the metal center is studied. We only focus on the Yttrium–guanidinate interaction.

The obtained values are reported in Table 4 (Fig. 2). This analysis has been performed for all the investigated complexes, and the results are reported in (SI. 2). The ratio of electrostatic and orbital energies, as obtained by this method can give an approximate measurement of the covalency degree in the metal–ligand bonding (Lein et al., 2003). In Table 4 the E_{ele}/E_{orb} ratio indicates a majority of ionic bonding can be well confirmed by analyzing Fig. 2. It is found that all E_{pauli} are destabilizing, whereas E_{ele} largely predominates, which is in agreement with the ionic character of dissociation. Bond dissociation energies (BDE) of the Y-gun bonding are slightly increased by increasing the alkyl group and in particular the Ny position, the bonding is found to be stabilized in this position from approximately 2 eV compared to N_c. The variation of the electrostatic component also follows the same variation than BDE, is found to be increased by approximately 3 eV.

3.5. Vibrational frequencies

The calculations of vibration frequencies show that these models are all located at the stable minimal points of the potential energy surfaces. They are all therefore stable complexes.

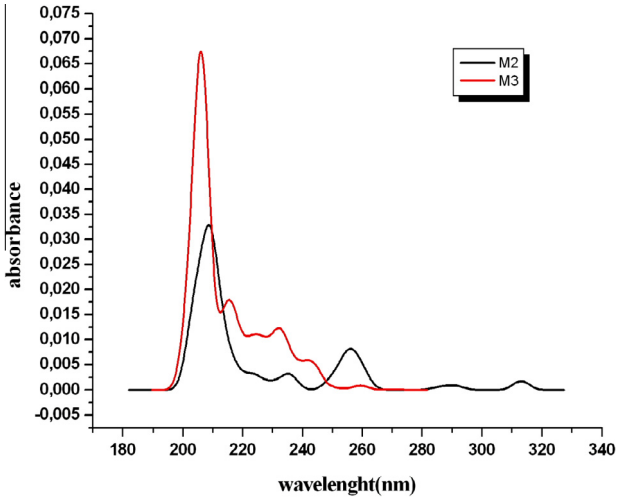

Figure 4 Theoretical UV–vis absorption spectra of M2 and M3 complexes.

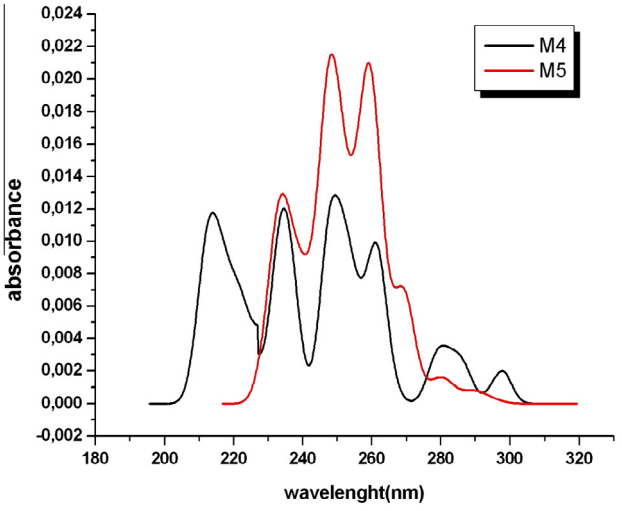

Figure 5 Theoretical UV–vis absorption spectra of M4 and M5 complexes.

Fig. 3 presents a predicted IR spectrum determined from theoretical calculations of some of these models. The IR spectra of these complexes exhibit strong absorptions in the range of 1522–1538 cm^{-1} (1630–1640 cm^{-1} are the experimental values as obtained from Milanov et al. (2008)), which are consistent with a partial C═N double bond character.

3.6. UV/VIS spectroscopy

The optical properties of M2, M3, M4 and M5 have been theoretically investigated by means of TD DFT calculations. The absorption spectra reported in Figs. 4 and 5 are dominated in the UV–visible regions by absorption features at about 205–208, 231–234, 272–321 nm for M3 and M2 respectively and, 213–234, 234–248, 249–259, 261–280, 294–313 nm for M4 and M5, respectively, which are given in Table 5. The bands can be assigned to ICT (Intra charge transfer) and LMCT (Ligand to metal charge transfer). SI3 shows the plots of the most

Table 5 Computed excitation energies, electronic transition configurations and oscillator strengths (*f*) for the optical transitions of the absorption bands in the visible and near-UV region for the M2, M3, M4 and M5 in vacuum.

Excitation energy (eV)	Wave lengtht (nm)	Osc.strengtht (*f*)	Major contribution	Character
Model 2				
4.84	256.53	0.0200	(38%) HOMO−2 → LUMO + 5	LMCT
4.28	290.09	0.0020	(99%) HOMO−2 → LUMO + 1	ICT,LMCT
3.95	313.20	0.0070	(97%) HOMO−1 → LUMO	LMCT
3.93	321.36	0.00009	(97%) HOMO → LUMO	LMCT
Model 3				
4.55	272.56	0.0005	(99%) HOMO LUMO	ICT
Model 4				
4.89	249.72	0.0097	(50%) HOMO−1 → LUMO + 6	LMCT
4.08	313.20	0.0029	(82%) HOMO → LUMO	LMCT
Model 5				
5.28	234.38	0.0272	(70%) HOMO−3 → LUMO + 5	LMCT
4.98	248.61	0.00170	(57%) HOMO−1 → LUMO + 7	LMCT
4.42	280.27	0.00360	(62%) HOMO → LUMO + 3	LMCT
4.03	294.00	0.00011	(99%) HOMO → LUMO	ICT

representative molecular frontier orbitals in the ground states of M2, M3, M4, M5 respectively. The main difference in the absorption spectra of these four compounds is that ICT transition of M3 and M5 are strongly hypsochromically shifted compared with those of M2 and M4 respectively. The effect of the substituted position influences the HOMO–LUMO transition nature and this transition is of a character LMCT for N_Y position and their delocalization effect compared to that of N_C position which is attributed to their lower HOMO–LUMO gap value.

4. Conclusion

In this study, an investigation of the electronic structures of Yttrium tri-guanidinates complexes, based on DFT calculations, was performed for the first time. The distorted trigonal prism structure was found in all series, with the highest torsion angles obtained for substitution in the N_Y position. This angle varies between 16° and 18° in the synthesized compounds, its value attains 21.2° in the M4 ($Y[(N_YR)_2CN_CR_1R_2]_3$; R = Et, R_1 = R_2 = H).

The energy decomposition analysis indicates a majority ionic bonding in all systems and that the substitution in the N_Y position increases the degree of covalency in the bonding.

The TDDFT calculations reveal that the substituted position influences the HOMO–LUMO transition nature, these transitions are of a LMCT character for N_Y position and are bathochromically and strongly hypochromically shifted compared to those of the N_C position.

Acknowledgements

The authors are very thankful to the « Université Lyon 1 and CNRS UMR 5180 Sciences Analytiques; Laboratoire de Chimie Physique Théorique, bâtiment Dirac, 43 boulevard du 11 Novembre 1918, 69622 Villeurbanne Cedex (France) » for offering the computing facilities and helpful discussion with the scientists. Also, the authors like to thank Prof Jawwad A. Darr, Professor of Materials Chemistry, Clean Materials Technology Group, Department of Chemistry, University College London, UCL, 20 Gordon Street, London WC1H 0AJ, United Kingdom, for reading and giving fruitful advice in improving the English and Scientific content of the manuscript.

Appendix A. Supplementary data

Supplementary data associated with this article can be found, in the online version, at http://dx.doi.org/10.1016/j.arabjc.2013.03.004.

References

Ajellal, N., M.Lyubov, D., Sinenkov, M.A., 2008. Chem. Eur. J. 14 (18), 5440, DOI: 10.1002/chem.200800288.

Bickelhaupt, F.M., Baerends, E.J., 2000. Rev Comput Chem, In: Lipkowitz, K.B., Boyd, D.B. (Eds.), vol. 15, Wiley-VCH, New York, pp. 1–86.

Bickelhaupt, F.M., Baerends, E.J., 2000. Rev Comput Chem. In: Lipkowitz, K.B., Boyd, D.B. (Eds.), vol. 15. Wiley-VCH, New York.

Chen, J.L., Yao, Y.M., Luo, Y.J., Zhou, L.Y., Zhang, Y., Shen, Q.J., 2004. Organomet. Chem. 689 (6), 1019, DOI:10.1016/j.jorganchem.2003.12.041.

Ge, S.Z., Meetsma, A., Hessen, B., 2008. Organometallics 27 (13), 3131, DOI: 10.1021/om800032g.

Giesbrecht, G.R., Whitener, G.D., Arnold, J., 2001. J.Chem. Soc. Dalton Trans. 2001 (6), 923, DOI: 10.1039/B008164G.

Hirshfeld, F.L., 1977. Theor. Chim. Acta 44 (2), 129, DOI: 10.1007/BF00549096.

Lein, M., Szabo, A., Kovacs, A., Frenking, G., 2003. Faraday Discuss. 124, 365, DOI: 10.1039/B300066B.

Luo, Y., Yao, Y., Shen, Q., 2002. Macromolecules 35, 8670, DOI: 10.1021/ma0211380.

Milanov, A.P., Fischer, R.A., Devi, A., 2008. Inorg. Chem. 47 (23), 11405, DOI: 10.1021/ic801432b.

Milanov, A.P., Thiede, T.B., Devi, A., Fischer, R.A., 2009. J. Am. Chem. Soc. 131 (47), 17062, DOI: 10.1021/ja907952g.

Pang, X., Sun, H., Zhang, Y., Shen, Q., Zhang, H., 2005. Eur. J. Inorg. Chem. 2005 (8), 1487.

Perdew, J.P., Chevary, J.A., Vosko, S.H., Jackson, K.A., Pederson, M.R., Singh, D.J., Fiolhais, C., 1992. Phys. Rev. B 46, 6671, DOI:10.1103/PhysRevB.46.6671.

Skvortsov, G.G., Yakovenko, M.V., Fukin, G.K., Cherkasov, A.V., Trifonov, A.A., 2007. Russ. Chem. Bull. Int. Ed. 56 (9), 1742, DOI: 10.1007/s11172-007-0270-2.

Trifonov, A.A., Skvortsov, G.G., Lyubov, D.M., Skorodumova, N.A., Fukin, G.K., Baranov, E.V., Glushakova, V.N., 2006. Chem. Eur. J 12 (20), 5320, DOI: 10.1002/chem.200600058.

van Lenthe, E., Ehlers, A., Baerends, E.J., 1999. J. Chem. Phys. 110, 8943, DOI:10.1063/1.478813.

Wang, Dongqi, Zhao, Cunyuan, Phillips David, Lee, 2004. Organometallics 23 (8), 1953.

Yao, Y., Luo, Y., Chen, J., Zhang, Z., Zhang, Y., Shen, Q., 2003. J. Organomet. Chem. 679 (2), 229, Doi: 10.1016/S0022-32X(03)00600-4.

Zhou, L., Yao, Y., Zhang, Y., Xue, M., Chen, J., Shen, Q., 2004. Eur. J. Inorg. Chem. 2004 (10), 2167, DOI: 10.1002/ejic.200300856.

Zhou, L., Yao, Y., Zhang, Y., Sheng, H., Xue, M., Shen, Q., 2005. Appl. Organomet. Chem. 19 (3), 398, DOI: 10.1002/aoc.855.

Ziegler, T., Rauk, A., 1979. Inorg. Chem. 18 (6), 1558, DOI: 10.1021/ic50196a034.